

## MIT Open Access Articles

### *Karhunen-Loeve representation of stochastic ocean waves*

The MIT Faculty has made this article openly available. **Please share** how this access benefits you. Your story matters.

**Citation:** Sclavounos, P. D. Karhunen-Loeve Representation of Stochastic Ocean Waves. Proceedings of the Royal Society A: Mathematical, Physical and Engineering Sciences 468, no. 2145 (July 27, 2012): 2574-2594.

**As Published:** <http://dx.doi.org/10.1098/rspa.2012.0063>

**Publisher:** Royal Society

**Persistent URL:** <http://hdl.handle.net/1721.1/79364>

**Version:** Author's final manuscript: final author's manuscript post peer review, without publisher's formatting or copy editing

**Terms of use:** Creative Commons Attribution-Noncommercial-Share Alike 3.0



# **Karhunen-Loeve Representation of Stochastic Ocean Waves**

By Paul D. Sclavounos

Department of Mechanical Engineering  
Massachusetts Institute of Technology

September 2011

## **Abstract**

A new stochastic representation of a seastate is developed based on the Karhunen-Loeve spectral decomposition of stochastic signals and the use of Slepian Prolate Spheroidal Wave Functions with a tunable bandwidth parameter. The new representation allows the description of stochastic ocean waves in terms of a few independent sources of uncertainty when the traditional representation of a seastate in terms of Fourier series requires an order of magnitude more independent components. The new representation leads to parsimonious stochastic models of the ambient wave kinematics and of the nonlinear loads and responses of ships and offshore platforms. The use of the new representation is discussed for the derivation of critical wave episodes, the derivation of up-crossing rates of nonlinear loads and responses and the joint stochastic representation of correlated wave and wind profiles for use in the design of fixed or floating offshore wind turbines. The forecasting is also discussed of wave elevation records and vessel responses for use in energy yield enhancement of compliant floating wind turbines.

## 1. Introduction

The design of ships and offshore structures that are expected to withstand severe storms and operate safely over a period of several decades requires an assessment of their structural reliability against extreme wave loads and fatigue. Ocean waves and the responses of marine structures are usually modeled as stationary Gaussian random processes represented by stochastic Fourier series based on the work of Rice (1944, 1945). The standard stochastic model of a seastate assumes that the free surface elevation may be represented by the superposition of a large number of Fourier components, typically 20-50 depending on the application, with random and independent phases drawn from the uniform distribution and amplitudes determined from the power spectral density of the seastate [Ochi (1998)]. The use of a seastate representation with a large number of independent sources of uncertainty in nonlinear wave body interactions leads to a computational task which may become prohibitively expensive when the statistics of extreme loads and responses are necessary. Therefore a representation of the seastate with the smallest possible number of independent sources of uncertainty would be very beneficial. When coupled with theoretical models of the nonlinear wave loads explicit expressions for the nonlinear probability density functions and threshold up-crossing rates become possible. The significance of a representation of linear and nonlinear random signals in terms of a small number of independent canonical components is discussed by Kac and Siegert (1947) and Wiener (1958).

Sines and cosines are but one of all possible orthogonal basis function sets that may be used for the representation of deterministic or stochastic signals in the form of a series with stochastic coefficients. Given the power spectral density of the signal an optimal orthogonal set of basis functions exists that fits the signal with the minimum number of independent sources of uncertainty. This basis set follows from the spectral decomposition theorems of Loeve (1945) and Karhunen (1947) [see Basilevsky (1994)]. An eigenvalue-eigenfunction problem is formulated and cast in the form of an integral equation of the first kind with a kernel equal to the autocorrelation function of the signal. The solution of this integral equation allows the representation of the signal as the linear superposition of the eigenfunctions multiplied by independent random variables with variance equal to the corresponding eigenvalues. A rapid decay of the eigenvalues indicates that a small number of independent components are sufficient

for the stochastic representation of the signal. This is indeed the case for narrow banded seastates for which less than three to five terms in the Karhunen-Loeve representation may provide sufficient accuracy.

The solution of the Karhunen-Loeve (KL) eigenvalue problem is a complex task and analytical solutions are available only in a few special cases. Such a case was considered by Slepian and Pollack (1961) and involves the *sinc* ( $\sin x/x$ ) function as the kernel in the KL integral equation. The eigenfunctions turn out to be the Prolate Spheroidal Wave Functions (PSWF) which form an orthonormal basis set with properties analogous to those of Fourier series, Chebyshev and Legendre polynomials. A distinct advantage of PSWFs is that they can be maximally concentrated in a given interval via the selection of a controllable bandwidth parameter known as the Slepian frequency. Moreover, they have the attractive property that they are invariant to a finite and infinite Fourier transform. Their application in communication theory is discussed by Moore and Cada (2004) and their mathematical properties and computation is presented in Xiao, Rockhlin and Yarvin (2001).

Drawing upon the properties of PSWFs a general solution of the Karhunen-Loeve integral equation is developed in the present article. The kernel is given by the autocorrelation function of a stationary seastate with a known spectrum. The KL integral equation of the first kind is reduced to a spectral matrix eigenvalue problem which accepts an efficient solution. For narrow banded seastates a rapid decay of the eigenvalues is observed. The number of dominant components in the Karhunen-Loeve-Slepian (KLS) representation depends on the magnitude of a tunable bandwidth parameter known as the Slepian frequency. Its selection for specific applications is discussed and its magnitude is found to depend on the bandwidth of the spectrum and the time scale of the memory effects in the wave-body interaction problem under consideration.

The use of the KLS representation of a seastate is discussed in connection with a recent theoretical nonlinear wave load model developed by Sclavounos (2011) which permits the derivation of explicit expressions for the extreme statistics for use in design. The use of the KLS representation for the design of a critical wave episode in a seastate is also described. The

extension of the present solution methodology to the joint KL representation of correlated stochastic ocean wave elevations and wind speed profiles is addressed. The KL representation of stochastic wind speeds and loads on wind turbines may be derived along lines similar to those for stochastic waves. The fundamental orthonormal basis set for averaged wind speeds differs from the PSWFs and may also be derived in explicit form from an analytical approximation of the wind speed autocorrelation function. This enables the derivation of a parsimonious joint KL representation of the wave loads on the floaters and wind loads on the turbine for use in the study of extremes and fatigue loads.

The Karhunen-Loeve representations of ocean waves, the responses of floating bodies and the wind speeds and loads on wind turbines may be used to generate accurate short-term forecasts of the respective quantities. Such forecasts may be generated in real time and used for the safe operation of ships and offshore platforms in severe seastates. Short-term forecasts of wind speeds coupled with feed-forward blade pitch control strategies may be used to mitigate loads on the blades and increase the energy yield of multi-megawatt onshore and offshore wind turbines. Analogous forecasts of the responses of floating wind turbines may be used to convert part of the kinetic energy of the floater imparted by the waves into wind energy via bladed pitch control strategies. Finally forecasts of ocean wave elevations and of the wave exciting forces on floaters are known to be essential for the design of efficient wave energy converters.

## 2. Spectral Decomposition of Stochastic Wave Records

Consider a wave elevation record  $\zeta(X, Y, t)$  from a stationary and ergodic seastate where  $(X, Y, Z)$  is an earth fixed coordinate system with  $Z=0$  being the calm water surface and with the positive  $Z$ -axis pointing upwards. The wave record measured at  $X=Y=0$  has the same statistical properties as the wave record measured at other  $(X, Y)$  locations. For the sake of brevity the following notation is adopted for the signal  $\zeta(t) \equiv \zeta(t, 0, 0)$ . The  $(X, Y, Z)$  coordinates are introduced again later in the article when the space-time dependence of the velocity potential corresponding to the seastate is derived.

The autocorrelation function of the signal is given by

$$(2.1) \quad R(\tau) = E[\zeta(t)\zeta(t+\tau)] = R(-\tau)$$

The expectation in (2.1) is taken over an ensemble of records at a fixed time  $t$  or over time for a single stationary record. For a stationary ergodic seastate the two definitions lead to an identical result. In practice the use of the temporal average is more convenient. It is hereafter assumed that  $R(\tau)$  is a known deterministic even function of the time lag  $\tau$ . The two-sided power spectral density of the signal  $\zeta(t)$  is the Fourier transform of the autocorrelation function. The following standard relations hold

$$(2.2) \quad \begin{aligned} S(\omega) &= \int_{-\infty}^{\infty} d\tau e^{-i\omega\tau} R(\tau) = S(-\omega) \\ R(\tau) &= \frac{1}{2\pi} \int_{-\infty}^{\infty} d\omega e^{i\omega\tau} S(\omega) \\ \sigma^2 = R(0) &= \frac{1}{2\pi} \int_{-\infty}^{\infty} d\omega S(\omega) = \int_0^{\infty} d\omega S_{\zeta}(\omega) \\ S_{\zeta}(\omega) &= \frac{1}{\pi} S(\omega), \quad \omega > 0 \end{aligned}$$

In (2.2) the standard deviation of the signal  $\sigma$  is also defined in terms of the one-sided wave spectrum  $S_\zeta(\omega)$  which accepts a number of standard parametrizations in ocean engineering discussed in Ochi (1998).

Consider a signal over a finite time interval  $(-T, T)$ . The Karhunen-Loeve theorem states that  $\zeta(t)$  accepts the expansion

$$(2.3) \quad \zeta(t) = \sum_{n=0}^{\infty} \alpha_n f_n(t), \quad -T < t < T$$

Assuming that  $\zeta(t)$  is a stochastic process, the coefficients  $\alpha_n$  are independent random variables such that

$$(2.4) \quad \begin{aligned} E(\alpha_n^2) &= \kappa_n \\ E(\alpha_m \alpha_n) &= 0, \quad m \neq n \end{aligned}$$

The deterministic functions  $f_n(t)$  are solutions of an eigenvalue problem cast in the form of an integral equation of the first kind with the autocorrelation function as its kernel

$$(2.5) \quad \begin{aligned} \int_{-T}^T R(t-\tau) f_n(\tau) d\tau &= \kappa_n f_n(t), \quad n = 0, \dots \\ \int_{-T}^T f_m(\tau) f_n(\tau) d\tau &= \begin{cases} 1, & m = n \\ 0, & m \neq n \end{cases} \\ R(t-\tau) &= \sum_{n=0}^{\infty} \kappa_n f_n(t) f_n(\tau) \\ R(t) &= \sum_{n=0}^{\infty} \kappa_n f_n(0) f_n(t) \\ \sigma^2 = R(0) &= \sum_{n=0}^{\infty} \kappa_n f_n^2(0) \\ \alpha_n &= \int_{-T}^T \zeta(t) f_n(t) dt \end{aligned}$$

A number of observations follow from the KL stochastic series expansion (2.3)-(2.5):

- The independent random variables  $\alpha_n$  are Gaussian if the signal  $\zeta(t)$  is Gaussian which is often the case with ocean waves. Yet the expansion applies to non-Gaussian signals.
- The eigenfunctions  $f_n(t)$  are even and odd functions for positive and negative values of their argument in the range  $(-T, T)$ . They are obtained from the solution of the eigenvalue problem derived below.
- The rate of decay of the eigenvalues  $\kappa_n$  with increasing  $n$  suggests the number of terms that are sufficient to keep in the stochastic series expansion (2.3). If this number is small the signal is governed by a small number of independent sources of uncertainty with statistical properties given by (2.3)-(2.5).
- The basis set  $f_n(t)$  is optimal in the sense that it allows the representation of the autocorrelation function with the minimum number of terms in the series in the third equation of (2.5).
- The KL representation maximizes the Shannon entropy measure which reveals the minimum number of terms that are sufficient for the representation of the variability of the signal.

These and other optimality properties of the KL representation are discussed in Basilevsky (1994).

The analytical determination of the eigenfunctions and eigenvalues corresponding to the autocorrelation function of the signal is a non-trivial task. A general solution that applies to ocean waves and other signals with known power spectral densities and autocorrelation functions is developed in the next section.



### 3. Solution of the Karhunen-Loeve Integral Equation

The autocorrelation function of the signal introduced in (2.5) is seen to accept an expansion in terms of the eigenfunctions  $f_n(t)$  which however are yet unknown. These eigenfunctions should ideally have a shape similar to that of the autocorrelation function. Figure 1 plots the autocorrelation function of two seastates with significant wave heights  $H_s \approx 4\sigma$  equal to 6m and 10m, respectively.

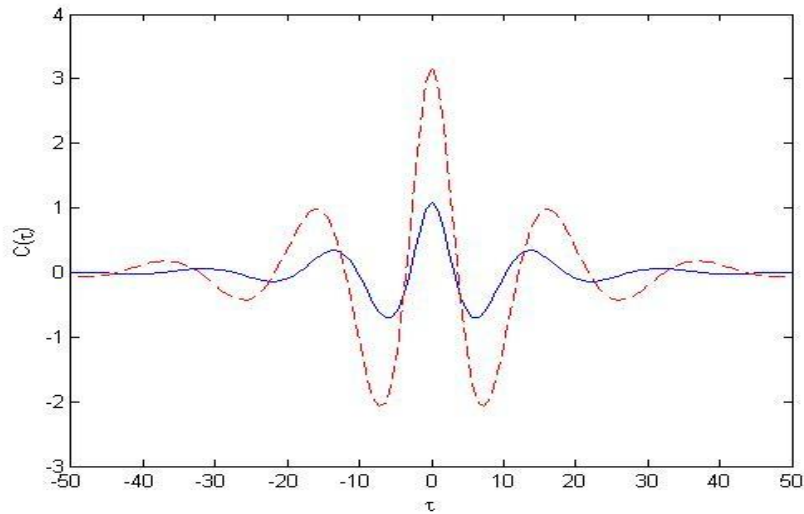


**Figure 1:** Seastate Autocorrelation functions:  $H_s=10\text{m}$  (Red Curve);  $H_s=6\text{m}$  (Blue curve)

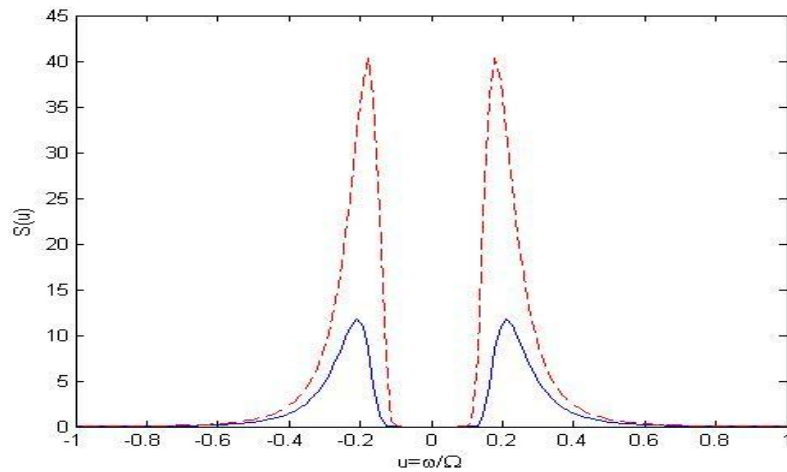


**Figure 2:** Spectral Densities of seastates with  $H_s=10\text{m}$  (Red Curve);  $H_s=6\text{m}$  (Blue curve)

Figure 3 plots the *sinc* function which is the autocorrelation function of a band limited signal with a power spectral density constant for  $-\Omega < \omega < \Omega$  and zero for  $|\omega| > \Omega$ . The *sinc* function shares strong similarities with the seastate autocorrelation function and will guide the derivation of the solution of (2.5) described below.

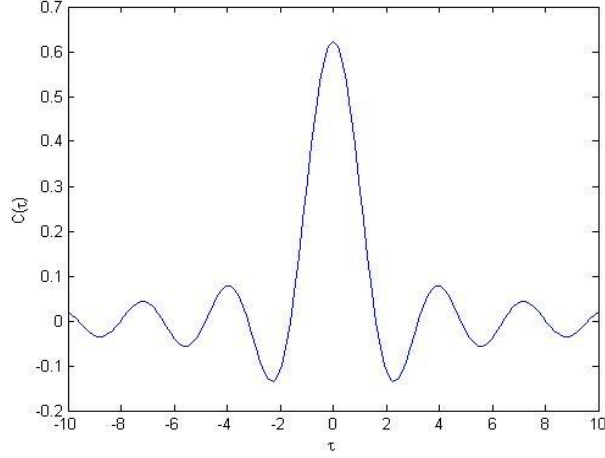


**Figure 3:** *Sinc* function  $C(\tau) = \frac{\sin \Omega \tau}{\pi \tau}$ ,  $\Omega = 2$

David Slepian observed that the eigenvalue problem (2.5) accepts an explicit solution when its kernel is the *sinc* function. This follows from the identity

$$(3.1) \quad \int_{-1}^1 \frac{\sin c(x-u)}{\pi(x-u)} \psi_n(u, c) du = \mu_n(c) \psi_n(x, c), \quad x = \frac{t}{T}, \quad c = \Omega T, \quad -T < t < T$$

The eigenfunctions are the Prolate Spheroidal Wave Functions (PSWFs)  $\psi_n(t, c)$  which satisfy the following relations [Xiao, Rokhlin and Yarvin (2001)]

$$(3.2) \quad \begin{aligned} \int_{-1}^1 \psi_n(u, c) e^{icxu} du &= \lambda_n(c) \psi_n(x, c), \\ \int_{-1}^1 \psi_m(u, c) \psi_n(u, c) du &= \begin{cases} 1, & m = n \\ 0, & m \neq n \end{cases} \\ e^{icxu} &= \sum_{j=0}^{\infty} \lambda_j \psi_j(x, c) \psi_j(u, c) \\ \frac{\sin c(x-u)}{\pi(x-u)} &= \sum_{j=0}^{\infty} \mu_j \psi_j(x, c) \psi_j(u, c), \quad \mu_j = \frac{c |\lambda_j|^2}{2\pi} \end{aligned}$$

The PSWFs  $\psi_n(u, c)$  form an orthonormal basis set in the interval  $(-1, 1)$ . They are symmetric functions of  $u$  for even values of  $n$  and anti-symmetric functions of  $u$  for odd values of  $n$ . The eigenvalues  $\lambda_n(c)$  are real for the even and purely imaginary for the odd PSWFs. The PSWFs depend parametrically on the bandwidth parameter  $c = \Omega T$  known as the Slepian frequency which controls the degree of their concentration within the interval  $(-1, 1)$ . The bandwidth parameter must be selected properly for each application a topic discussed in more detail below. The proper selection of the bandwidth parameter enlarges the space of available PSWFs introducing a flexibility not present in Fourier series.

The first equation in (3.2) shows that the PSWFs are invariant with respect to the finite Fourier transform. This Fourier invariance of the PSWFs proves very convenient in surface wave problems since it permits the transition from time to frequency domain representations using the same basis set. This property will be used later in the article to derive the velocity potential and flow kinematics of a seastate starting from the representation of the free surface elevation as the stochastic signal. Another property of PSWFs is that they decay at infinity for a large value of their argument at a rate that depends on the value of the bandwidth parameter  $c$ . This permits their use as an ambient wave signal that starts and ends with a calm free surface. This is an attractive property in numerical simulations carried out over time window  $(-T, T)$  of finite duration that circumvents the need for an artificial ramp up of the computation. The decay of PSWFs at infinity also permits their use with conservation theorems that make use of the assumption that the ambient seastate and the radiation-diffraction disturbances generated by floating bodies decay at infinity [Sclavounos (2011)].

The PSWFs are used next to solve the Karhunen-Loeve integral equation for a general two-sided power spectral density. This solution is used in the next section to generate a representation of a seastate and its associated velocity potential in terms of a small number of independent sources of uncertainty.

The third equation in (3.2) is a key addition theorem which allows the representation of the complex exponential in terms of a series of products of PSWFs. Its introduction in the definition of the autocorrelation function allows the reduction of the kernel of the KL integral equation into

a separable form which opens the way for the derivation of a symmetric matrix eigenvalue problem.

$$\begin{aligned}
R(t-\tau) &= \frac{1}{2\pi} \int_{-\infty}^{\infty} d\omega S(\omega) e^{i\omega(t-\tau)}, \quad -T < t, \tau < T, \quad c = \Omega T \\
(3.3) \quad &= \frac{1}{2\pi} \sum_{j=0}^{\infty} \lambda_j \psi_j\left(\frac{t}{T}, c\right) \int_{-\infty}^{\infty} d\omega S(\omega) \psi_j\left(\frac{\omega}{\Omega}, c\right) e^{-i\omega\tau} \\
&= \sum_{j=0}^{\infty} \lambda_j \psi_j\left(\frac{t}{T}, c\right) \phi_j(\tau) \\
\phi_j(\tau) &= \frac{1}{2\pi} \int_{-\infty}^{\infty} d\omega S(\omega) \psi_j\left(\frac{\omega}{\Omega}, c\right) e^{-i\omega\tau}
\end{aligned}$$

The third equation in (3.3) provides a series expansion of the autocorrelation function in terms of PSWFs and the function  $\phi_j(\tau)$ . This series allows the conversion of the convolution kernel into a separable one that is tractable analytically. Introducing the third equation of (3.3) in the Karhunen-Loeve integral equation (2.5) we obtain

$$(3.4) \quad \sum_{j=0}^{\infty} \lambda_j \psi_j\left(\frac{t}{T}, c\right) \int_{-T}^T f_n(\tau) \phi_j(\tau) d\tau = \kappa_n f_n(t)$$

Solving for the eigenfunctions  $f_n(t)$  in the right-hand side we obtain

$$\begin{aligned}
(3.5) \quad f_n(t) &= \sum_{j=0}^{\infty} A_j^n \psi_j\left(\frac{t}{T}, c\right) \\
A_j^n &= \frac{\lambda_j}{\kappa_n} \int_{-T}^T f_n(\tau) \phi_j(\tau) d\tau
\end{aligned}$$

The eigenfunctions are cast in the form of a series of PSWFs with yet unknown coefficients  $A_j^n$ .

Introducing this series expansion on both sides of (3.4) we obtain

$$(3.6) \quad \sum_{j=0}^{\infty} \lambda_j \psi_j\left(\frac{t}{T}, c\right) \int_{-T}^T \left[ \sum_{k=0}^{\infty} A_k^n \psi_k\left(\frac{\tau}{T}, c\right) \right] \phi_j(\tau) d\tau = \kappa_n \sum_{j=0}^{\infty} A_j^n \psi_j\left(\frac{t}{T}, c\right)$$

Both sides of (3.6) involve a series summation over the PSWFs  $\psi_j\left(\frac{t}{T}, c\right)$ . Multiplying both sides with the PSWF  $\psi_i\left(\frac{t}{T}, c\right)$ , integrating over the interval  $-T < t < T$  and invoking their orthogonality from (3.2) we obtain

$$(3.7) \quad \lambda_i \sum_{k=0}^{\infty} A_k^n D_{ki} = \kappa_n A_i^n$$

$$D_{ki} = \int_{-T}^T \psi_k\left(\frac{\tau}{T}, c\right) \phi_i(\tau) d\tau$$

Invoking the definition of  $\phi_i(\tau)$  from (3.3) it follows that

$$(3.8) \quad \begin{aligned} D_{ki} &= \int_{-T}^T \psi_k\left(\frac{\tau}{T}, c\right) \phi_i(\tau) d\tau \\ &= \frac{1}{2\pi} \int_{-T}^T \psi_k\left(\frac{\tau}{T}, c\right) \left[ \int_{-\infty}^{\infty} d\omega S(\omega) \psi_i\left(\frac{\omega}{\Omega}, c\right) e^{-i\omega\tau} \right] d\tau \\ &= \frac{1}{2\pi} \int_{-\infty}^{\infty} S(\omega) \psi_i\left(\frac{\omega}{\Omega}, c\right) \left[ \int_{-T}^T \psi_k\left(\frac{\tau}{T}, c\right) e^{-i\omega\tau} d\tau \right] d\omega \\ &= \lambda_k^* c G_{ik} \\ G_{ik} &= \frac{1}{2\pi} \int_{-\infty}^{\infty} S(\omega) \psi_i\left(\frac{\omega}{\Omega}, c\right) \psi_k\left(\frac{\omega}{\Omega}, c\right) d\left(\frac{\omega}{\Omega}\right) \end{aligned}$$

In (3.8) the \* denotes the complex conjugate of the eigenvalue  $\lambda_k^*$  when it is purely imaginary for odd PSWFs. Substituting (3.9) in (3.8) we obtain a symmetric matrix eigenvalue problem of the form

$$(3.9) \quad \begin{aligned} [E] \vec{A} &= \kappa \vec{A} \\ E_{ik} &= \lambda_i \lambda_k^* c G_{ik} = E_{ki} \end{aligned}$$

The eigenvalues  $\kappa_n$  and corresponding eigenvectors  $A_i^n, i=0,1,2,\dots$  are indexed by  $n$  and provide the solution of the Karhunen-Loeve integral equation. The eigenfunctions are determined from (3.5)

The eigenvalue problem (3.9) consists of even and odd parts that are independent. This follows upon inspection of the elements of the matrix  $E_{ki}$ . Its elements are non zero only if  $(i,k)$  are either both even or both odd. If one is even and the other odd the last integral in (3.8) is identically zero by virtue of the symmetry of the spectral density  $S(\omega)$  with respect to its argument and the symmetry/anti-symmetry of the PSWFs of even/odd order, respectively. The even/odd eigenvalue problems correspond to the even/odd eigenfunctions  $f_n(t)$  by virtue of their definition in (3.5). The eigenvectors  $A_j^n$  follow from the solution of (3.9) for the even/odd problems respectively. The rate of decay of the eigenvalues  $\kappa_n$  determines the number of terms that are sufficient to keep in the Karhunen-Loeve series representation of the signal.

The elements of the matrix  $E_{ki}$  decrease with increasing  $(i,k)$  since the magnitude of the last integral in (3.8) decreases as  $(i,k)$  increase due to the oscillatory behavior of the PSWFs as their order increases. The eigenvalue problem (3.8) and (3.9) is well conditioned and its solution is straightforward using a standard matrix package and a subroutine for the evaluation of the PSWFs and their eigenvalues. Numerical results are presented in Section 5.

#### 4. Flow Kinematics of Karhunen-Loeve Seastate

The solution of the KLS integral equation leads to the representation of the free surface elevation at  $X=Y=0$  in the form

$$(4.1) \quad \begin{aligned} \zeta(t) &= \sum_{n=0}^{\infty} \alpha_n f_n(t), \quad -T < t < T \\ f_n(t) &= \sum_{j=0}^{\infty} A_j^n \psi_j\left(\frac{t}{T}, c\right) \end{aligned}$$

The coefficients  $\alpha_n$  are independent random variables with zero mean and variances  $\kappa_n$  given by the eigenvalues of the eigenvalue problem (3.9). The  $n$ -th basis function  $f_n(t)$  is seen from (4.1) to be a linear superposition of PSWFs with coefficients equal to the elements of the corresponding eigenvector. The series in the first equation of (4.1) includes both even and odd basis functions corresponding to even/odd PSWFs used in the second equation of (4.1) to represent the even and odd basis functions  $f_n(t)$ , respectively.

The representation (4.1) of the free surface elevation and the Fourier invariance of the PSWFs stated in (3.2) allows the direct representation of the velocity potential in the fluid domain corresponding to (4.1). Using (3.2) the second equation in (4.1) may be cast in the form

$$(4.2) \quad \begin{aligned} f_n(t) &= \sum_{j=0}^{\infty} A_j^n \psi_j\left(\frac{t}{T}, c\right) \\ &= \sum_{j=0}^{\infty} \frac{A_j^n}{\lambda_j} \lambda_j \psi_j\left(\frac{t}{T}, c\right) \\ &= \sum_{j=0}^{\infty} \frac{A_j^n}{\lambda_j} \int_{-1}^1 dx \psi_j(x, c) e^{ic\frac{t}{T}x}; \quad x = \frac{\omega}{\Omega}, c = \Omega T \\ &= \sum_{j=0}^{\infty} \frac{A_j^n}{\lambda_j \Omega} \int_{-\Omega}^{\Omega} d\omega \psi_j\left(\frac{\omega}{\Omega}, c\right) e^{i\omega t} \end{aligned}$$

The last equation in (4.2) expresses the free surface elevation corresponding to the basis function  $f_n(t)$  in terms of a Fourier integral over the frequency range  $-\Omega < \omega < \Omega$ . It is noted that the

eigenvalues  $\lambda_j$  are real for even PSWFs and purely imaginary for the odd PSWFs therefore the right-hand side of the last equation in (4.2) is always real.

Assuming a unidirectional seastate propagating in the positive X-direction, and invoking the linear dispersion relation, the velocity potential corresponding to the free surface elevation record  $f_n(t)$  takes the form

$$\begin{aligned}
 \phi_n(X, Z, t) &= \sum_{j=0}^{\infty} \frac{1}{\Omega} \int_{-\Omega}^{\Omega} d\omega \frac{ig\mathfrak{A}(\omega)}{\omega} e^{\frac{\omega^2}{g}Z} e^{i\omega t - i\frac{|\omega|}{g}X} \\
 \mathfrak{A}(\omega) &= \frac{A_j^n}{\lambda_j} \psi_j\left(\frac{\omega}{\Omega}, c\right) \\
 \varphi(X, Z, t; \omega) &= \frac{ig\mathfrak{A}(\omega)}{\omega} e^{\frac{\omega^2}{g}Z} e^{i\omega t - i\frac{|\omega|}{g}X} = \varphi^*(X, Z, t; -\omega)
 \end{aligned}
 \tag{4.3}$$

The velocity potential  $\phi_n(X, Z, t)$  is a linear superposition of plane progressive monochromatic wave components with amplitudes given by the second equation in (4.3). The last equation of (4.3) states that the velocity potential corresponding to each Fourier component is the complex conjugate of itself when the sign of the frequency is reversed. This property combined with the fact that the eigenvalues  $\lambda_j$  of even PSWFs are real while the eigenvalues of odd PSWFs are purely imaginary ensures that the velocity potential given by the first equation in (4.3) is a real quantity.

The velocity potential of the KLS representation of a stochastic seastate with elevation given by (4.1) follows in the form

$$\phi(X, Z, t) = \sum_{n=0}^{\infty} \alpha_n \phi_n(X, Z, t), \quad -T < t < T
 \tag{4.4}$$

This completes the derivation of the velocity potential of the seastate. The flow velocity follows by taking the gradient of (4.4) and the pressure follows from Bernoulli's equation.



## 5. Numerical Results

The numerical solution of the eigenvalue problem (3.9) was carried out with Matlab. The elements of the matrix  $E_{ki}$  involve the evaluation of integrals of the seastate spectral density multiplied by the product of two spheroidal wave functions and was carried out by quadrature. The integration is restricted to the range  $-\Omega < \omega < \Omega$  with the cut-off frequency  $\Omega$  selected to include the power spectral density band of pertinence to each application. The PSWFs and their eigenvalues  $\lambda_j$  were evaluated using the algorithms presented in Xiao, Rokhlin and Yarvin (2001).

A key attribute of the PSWFs as an orthonormal basis set is their parametric dependence on the parameter  $c = \Omega T$ . The proper selection of  $c$  for each application leads to the selection of PSWFs that lead to a rapid decay of the eigenvalues of (3.9), the minimum number of terms in the series expansion (4.1) and the minimum number of sources of uncertainty. In the case of the two seastate spectra plotted in Figure 2 the cut-off frequency was selected to be  $\Omega \simeq 0.6 \text{ rad / sec}$ .

The selection of the time window  $t \in (-T, T)$  depends on the type of response being studied. A seastate represented by a KLS expansion would be used as input in a time-domain numerical simulation of the nonlinear loads or responses of ships, offshore structures and fixed or floating wind turbines. The time window of the numerical simulation is typically selected so that transients of the response have died out and do not affect the useful part of the force or response simulation record. The time scale of transients is of the same order as the time scale of the memory effects of the load or response under consideration. The memory effects of the diffraction wave disturbance generated by the legs of offshore structures with diameters of 10-20m or the floaters of wind turbines with diameters of 5m are weak. Consequently, it is often sufficient to select the time window  $(-T, T)$  to be as wide as 2 wave periods. For a seastate modal period of  $T \simeq 12 \text{ sec}$ ,  $c = \Omega T \simeq 0.6 \times 12 = 7.2$ . The memory effects associated with of the responses of ships on the other hand are stronger and persist longer since ships are large volume structures. Therefore for wave load and ship response simulations the time window  $(-T, T)$  needs

to be 5-10 wave periods wide depending on the type of ship response of interest. For the same seastate modal period and cut-off frequency this leads to values of  $c = \Omega T \simeq 18-36$ . Consequently the PSWFs appropriate for each application have different bandwidth parameters  $c$ .

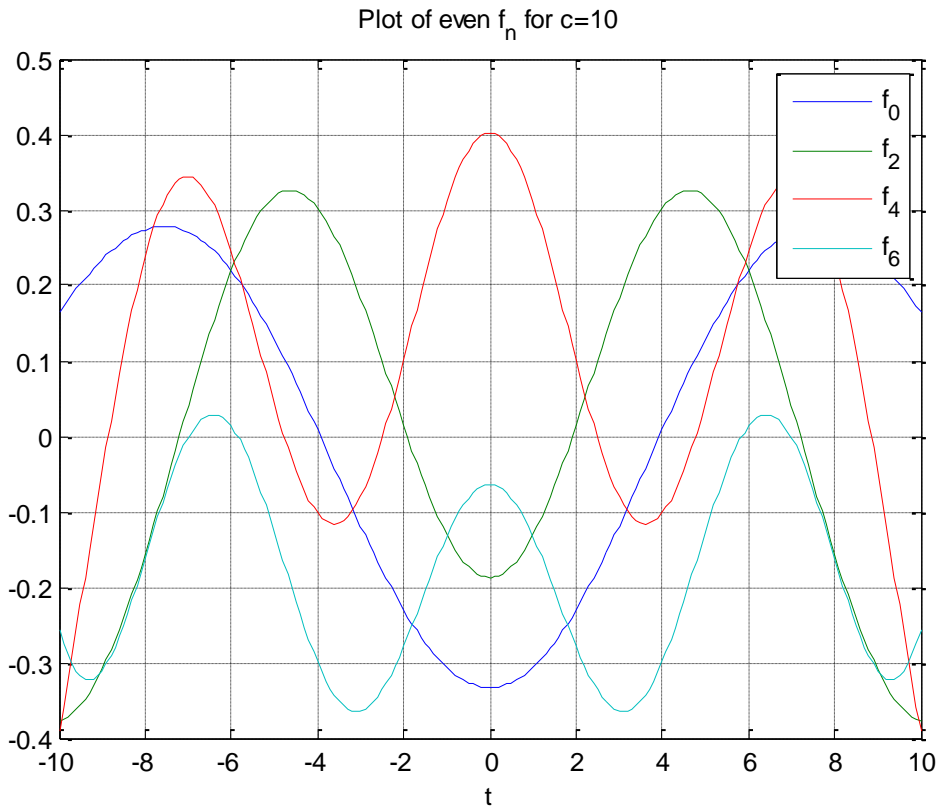


**Figure 4:** First four even basis functions for  $c=10$  [Eq. (4.1)]

Figures 4 and 5 plot the first four even and odd basis functions  $f_n(t)$  obtained from the solution of the eigenvalue problem (3.8) and (3.9). The power spectrum corresponds to a seastate with  $H_s=10\text{m}$  and peak period  $T_p=13.6$  and the value of the Slepian frequency is  $c=\Omega T=10$ .

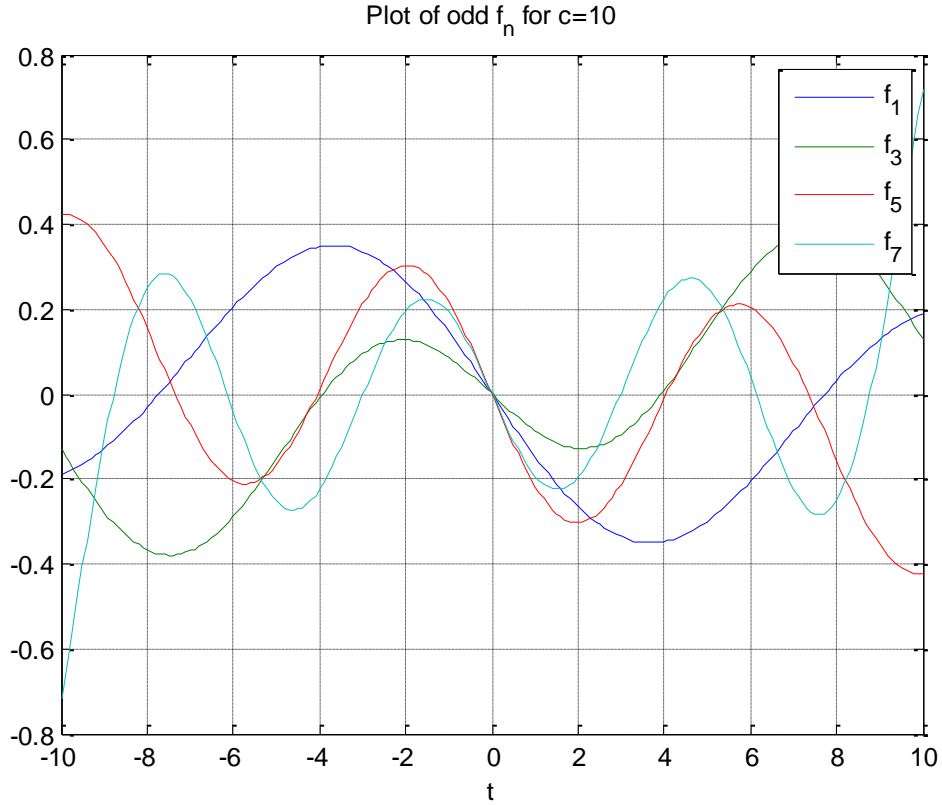


**Figure 5:** First four odd basis functions for  $c=10$  [Eq. (4.1)]

Figure 6 plots the autocorrelation function of the seastate and its expansion in terms of the even basis functions  $f_n(t)$  given by (2.5). It may be seen that 2-3 terms in the series (2.5) are sufficient for the accurate representation of the exact autocorrelation function. The rapid convergence of the KLS expansion is also shown in Figure 7 that plots the relative error of the variance of the signal given in (2.5) in the form of a KLS series of squares of the basis functions. It is seen that a 6% accuracy is achieved with three terms in the series and near perfect accuracy is achieved with four terms. The rate of decay of the even and odd eigenvalues is illustrated in Figure 8.

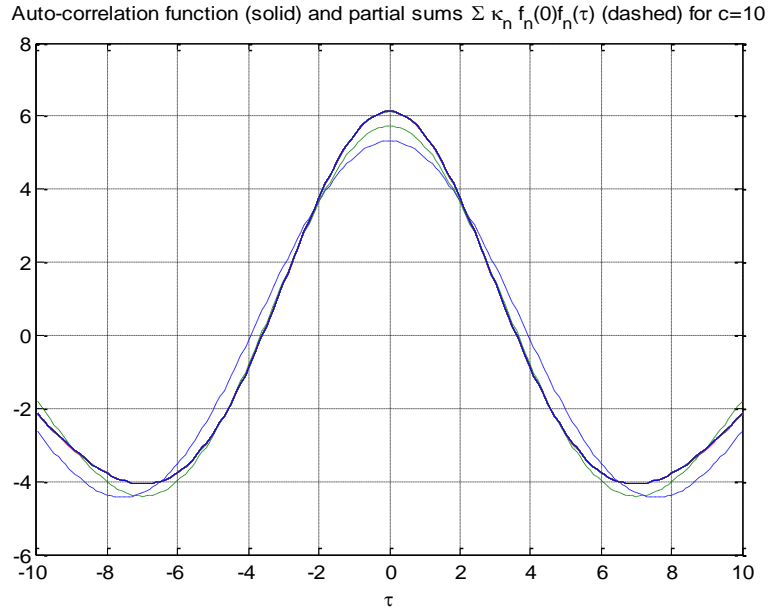


**Figure 6:** Autocorrelation function of seastate with  $H_s=10\text{m}$ ,  $T_p=13.6$  and  $c=10$

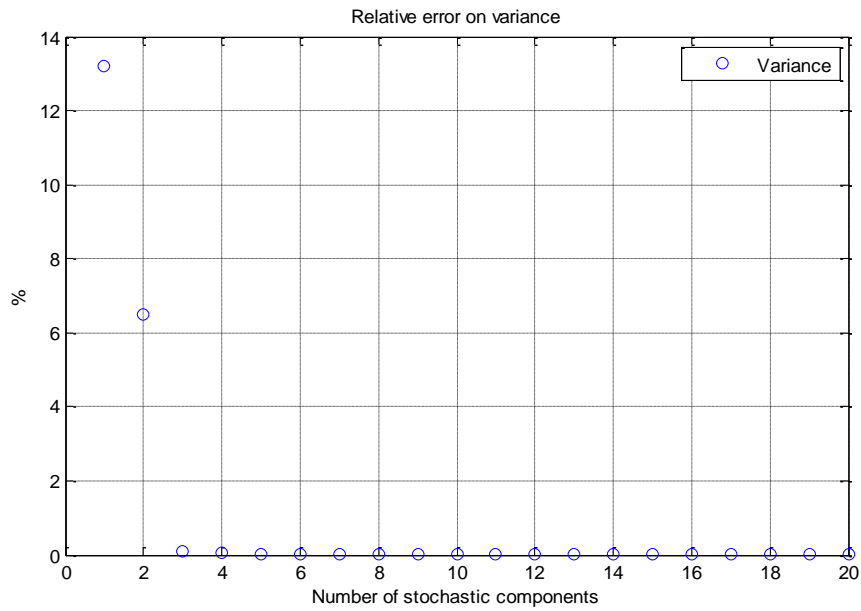


**Figure 7:** Variance of seastate elevation with  $H_s=10\text{m}$ ,  $T_p=13.6$  and  $c=10$

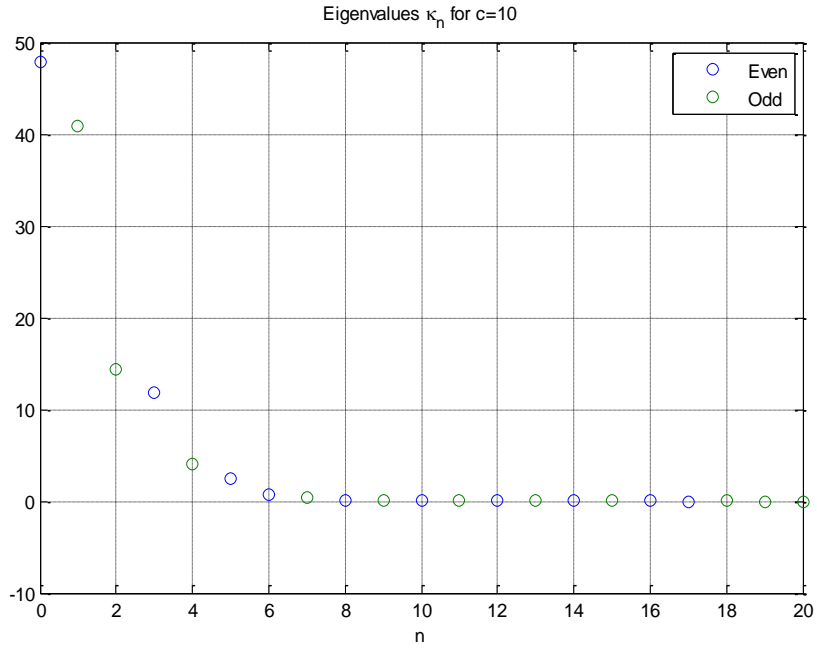


**Figure 8:** Rate of decay of even and odd eigenvalues for  $c=10$

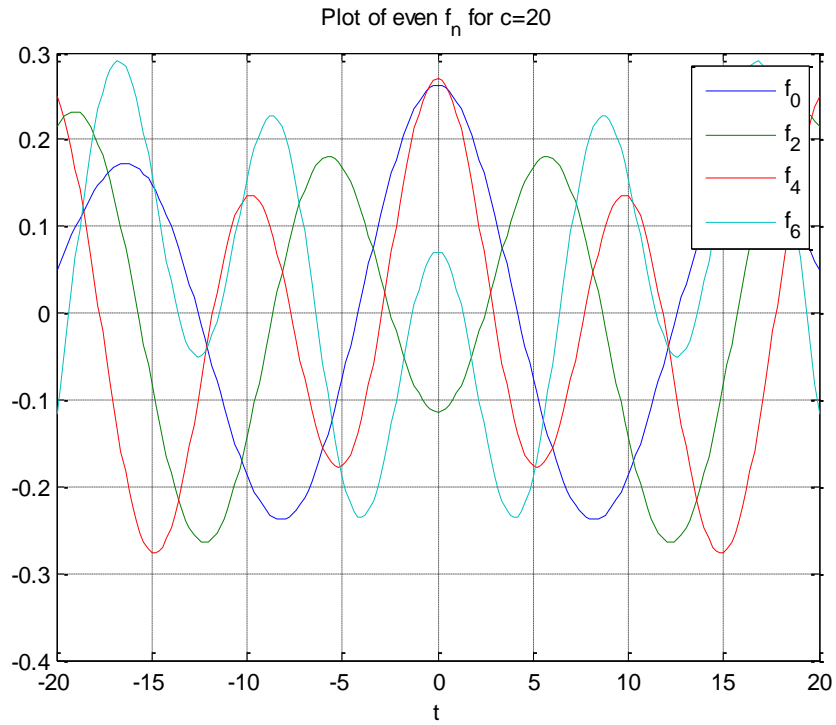


**Figure 9:** First four even basis functions for  $c=20$  [Eq. (4.1)]

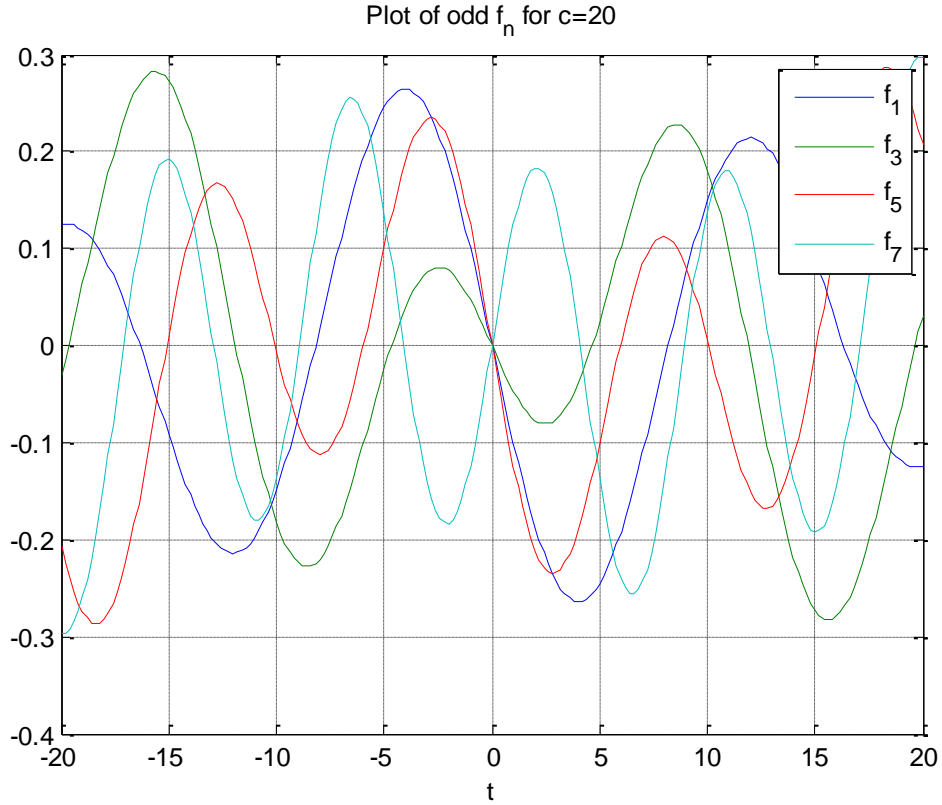


**Figure 10:** First four odd basis functions for  $c=20$  [Eq. (4.1)]

The corresponding results for a Slepian frequency  $c=20$ , the same cut-off frequency of  $\Omega=0.6$  rad/sec and twice as large a time window are shown in Figures 9-13. It is seen that the convergence of the KLS expansion is very fast and near perfect convergence of the variance is achieved with six terms in the series. The rate of convergence of the eigenvalues for the case with  $c=50$  corresponding to the same cut-off frequency and a time window of 100 sec is illustrated in Figure 14.

It may be observed from Figures 8, 13 and 14 that consecutive even and odd eigenvalues are nearly equal but not identical. In the Fourier series representation of a stochastic signal the random coefficients multiplying the even basis functions (cosines) and the odd basis functions (sines) have the same variance a consequence of the Pythagorean identity. This identity does not hold for the even and odd basis functions in the KLS series which are not periodic functions of time, a desirable property in simulations.

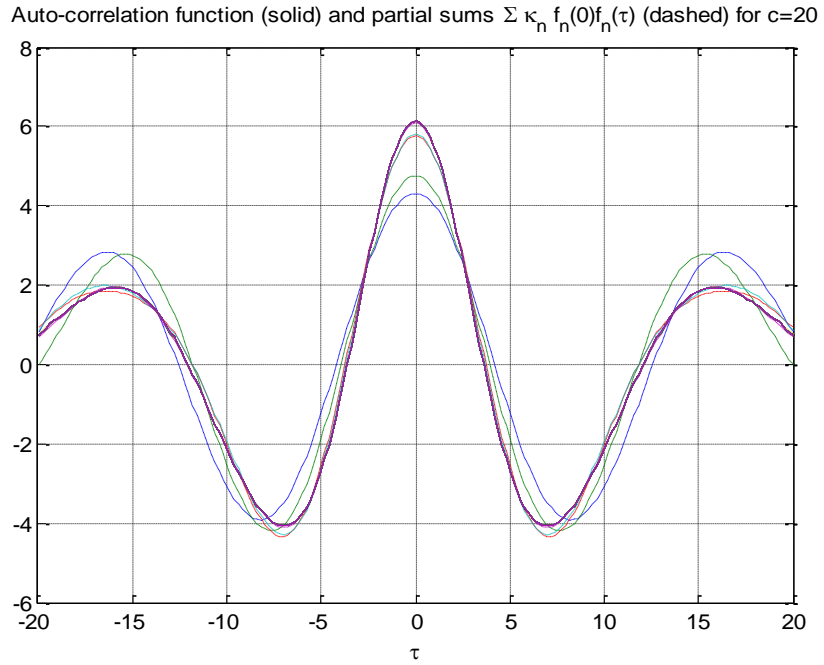


**Figure 11:** Autocorrelation function of seastate with  $H_s=10m$ ,  $T_p=13.6$  and  $c=20$

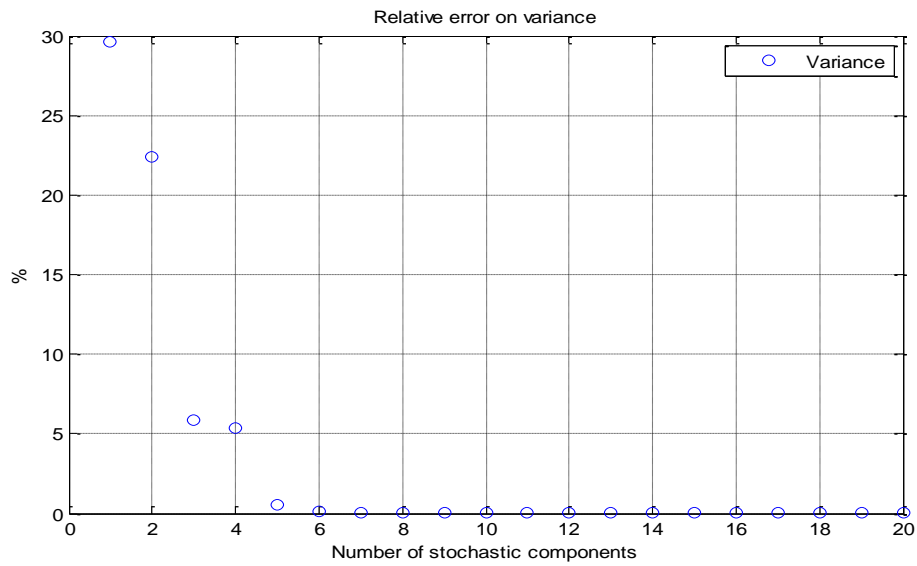


**Figure 12:** Variance of seastate elevation with  $H_s=10m$ ,  $T_p=13.6$  and  $c=20$

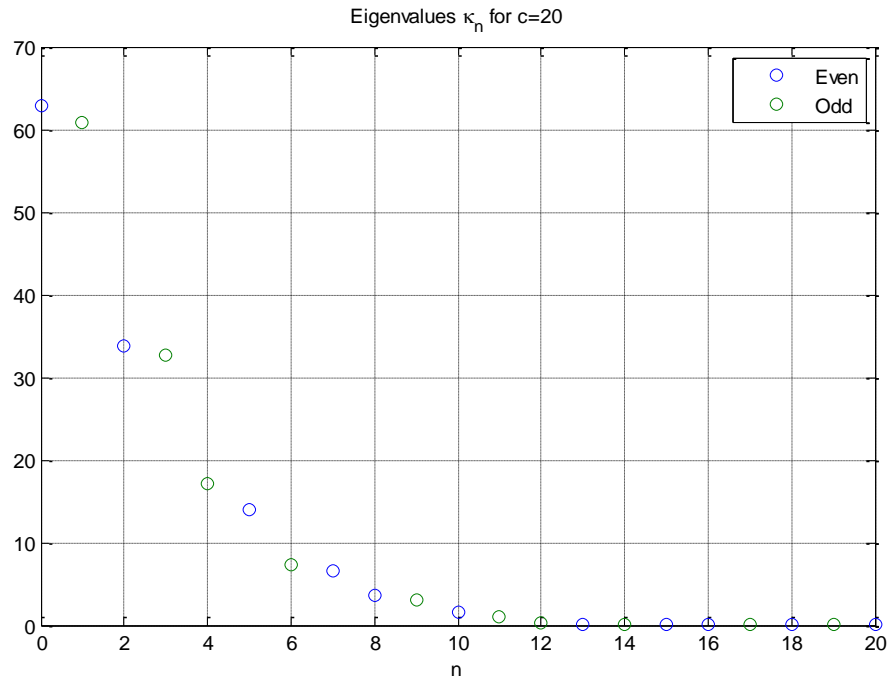


**Figure 13:** Rate of decay of even and odd eigenvalues for  $c=20$

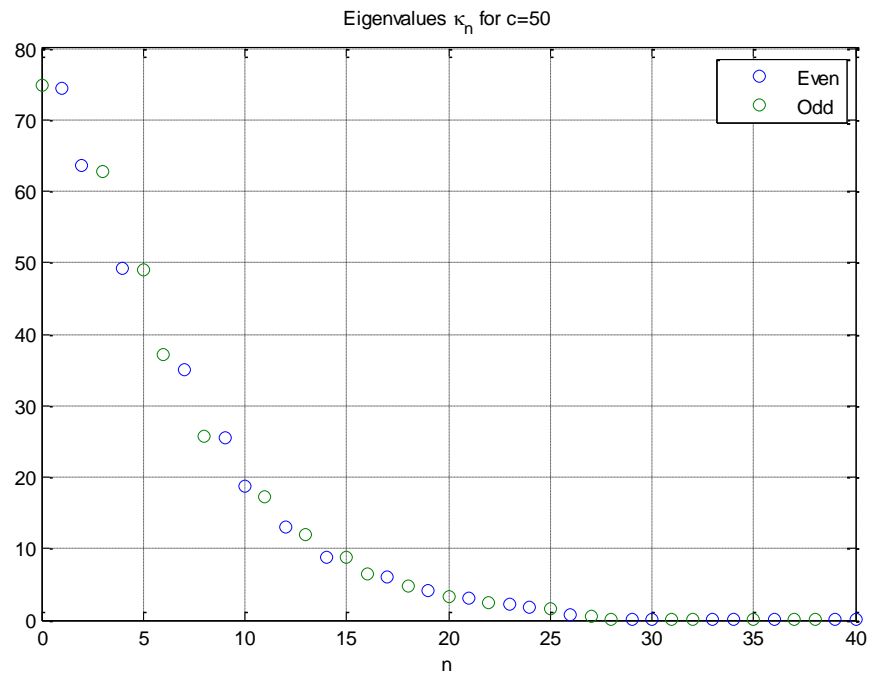


**Figure 14:** Rate of decay of even and odd eigenvalues for  $c=50$



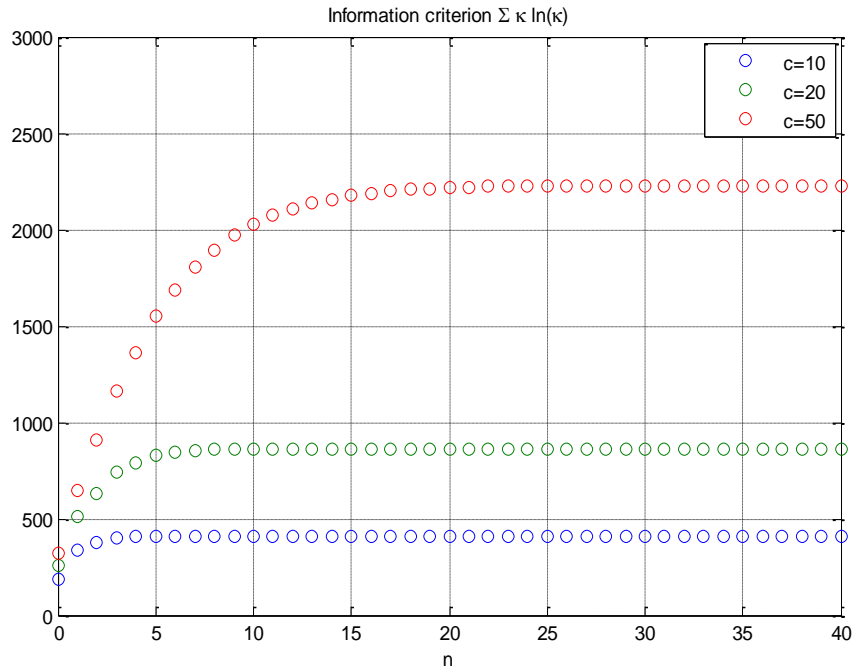


**Figure 15: Shannon Entropy Information Criterion**

An alternative measure of the variability of the signal is the Shannon entropy measure or Information Criterion. In the case of the KLS expansion it is given as the sum of the product of the eigenvalues times their natural logarithm. Figure 15 plots the Information Criterion as a function of the number of terms in the KLS series for three values of the Slepian frequency  $c$ . Convergence is achieved with  $n=3$ , 5 and 15 terms for  $c=10$ , 20 and 50 respectively. No more information about the variability of the signal is revealed by including more terms in the series.

## 6. Discussion

The Karhuenen-Loeve-Slepian representation of a seastate derived in this article enables the representation of the ocean environment with the minimum number of independent sources of uncertainty by selecting a tunable bandwidth parameter  $c$  optimally for each application. This representation proves particularly useful for the representation of critical wave episodes in a seastate and the study of the extreme statistics and threshold up-crossing rates of nonlinear loads and responses.

### Critical Wave Episodes

In a number of ocean engineering applications the derivation of the shape of a critical wave episode with a given amplitude is often of interest. This is often referred to as the Design Wave which may be used for the evaluation of the loads and responses of ships and offshore structures. Traditionally this wave is assumed to be a sinusoid with a large and prescribed amplitude. Yet this is often a conservative assumption and a more realistic representation is necessary.

Consider an ambient seastate with  $H_s=10\text{m}$  and  $T_p=13.6$ . The shape of the most probable Design Wave in such a seastate with a height  $H_d=20\text{m}$  may be readily determined from the KLS expansion. Assume that this wave will be used for the design of an offshore structure over a time window corresponding to a Slepian frequency of  $c=20$ . Without loss of generality the maximum wave height is assumed to occur at  $t=0$ . It follows from (4.1) that

$$(6.1) \quad \zeta(0) = H_d = \sum_{n=0}^3 \alpha_n f_n(0)$$

Four terms were kept in (6.1) leading to a 6% error in the KLS representation of the seastate elevation. The equality (6.1) enforces a linear constraint on the independent random variables  $\alpha_n$  which are assumed to be Gaussian with variances equal to the eigenvalues  $\kappa_n$ . Admissible values of  $\alpha_n$  therefore lie on a hyper plane in a four-dimensional space. The values of  $\alpha_n$  that lead to

the most probable Design Wave are the ones that maximize the joint Gaussian probability density function of  $\alpha_n$ ,  $n = 0, \dots, 3$

$$(6.2) \quad \max_{\alpha_n} [f(\alpha_0)f(\alpha_1)f(\alpha_2)f(\alpha_3)]; \quad H_d = \sum_{n=0}^3 \alpha_n f_n(0)$$

In (6.2)  $f(x)$  denotes the Gaussian probability density function and the independence of the  $\alpha_n$  has been invoked. The numerical solution of (6.2) for the values  $\alpha_n$  that maximize their joint density subject to the constraint (6.1) is a straightforward maximization problem. Substituting the values of  $\alpha_n$  obtained from the solution of (6.2) in (4.1) the shape of the Design Wave as a function of time is obtained. By definition it achieves its maximum value  $H_d$  at  $t=0$  and decays to zero for  $t<0$  and  $t>0$  when the even basis functions  $f_n(t)$  are expressed in terms of PSWFs as in (4.1). In this particular example the odd basis functions do not enter the definition of the Design Wave since their values vanish identically at  $t=0$ .

A similar approach may be used for other design studies where instead of the Design Wave other critical load episodes of interest in offshore applications are desired. The maximum likelihood estimation described above for the selection of the coefficients  $\alpha_n$  forms the basis of the First Order and Second Order Reliability methods (FORM & SORM) in structural design discussed in Kiureghian (2000) for linear and nonlinear problems.

## **Nonlinear Statistics of Loads and Responses**

In most applications of interest in offshore engineering the ambient seastate is assumed to be Gaussian. This is however not always an accurate assumption for the loads and responses of ships and offshore structures in severe seastates which exhibit significant departures from Gaussianity. Nonlinearities in the loads and responses affect their probability distributions which in turn affect significantly their extremes, threshold up-crossing rates and fatigue loads.

The literature on theoretical and computational models for the prediction of the nonlinear loads and responses of floating structures is extensive. Fully nonlinear simulations often lead to

prohibitive computational efforts when used in a stochastic seastate for the estimation of the statistics of extremes via Monte Carlo simulations. Therefore approximate methods are often used. Offshore structures typically consist of slender cylindrical members with diameters small compared to the wavelength of waves encountered in severe seastates. Ships are slender floating structures with beam and draft small compared to the wavelength of design waves. These geometric attributes justify the linearization of the radiation-diffraction wave disturbance due to the body about the ambient seastate profile which may be assumed to be nonlinear and with amplitude comparable to the characteristic dimension of the structure. This approximation was used by Scлавounos (2011) to derive compact expressions for the nonlinear time domain loads on ships and offshore structures that are explicit functions of the ambient seastate kinematics. Combined with a parsimonious KLS representation of the ambient seastate the stochastic nonlinear loads and responses may be expressed as quadratic and cubic functionals of a small number of random coefficients  $\alpha_n$  which are independent Gaussian random variables with variance  $\kappa_n$ . The probability density functions of quadratic or cubic functionals of  $\alpha_n$  are available in closed form in terms of their characteristic functions discussed by Kac and Siegert (1947) and Ochi (1998). This allows the derivation of explicit expressions of threshold up-crossing rates of extremes and fatigue loads for use in structural design discussed by Winterstein (1988).

An alternative approach often used for the study of the statistics of extremes is based on the derivation of the envelope of the process under consideration. In the case of the KLS representation of the free surface elevation given by (4.1), the envelope is obtained as the square root of the sum of the squares of the free surface elevation and its conjugate process defined as the Hilbert transform of the free surface elevation. The Hilbert transform of the basis functions  $f_n(t)$  is a linear combination of the Hilbert transform of the PSWFs. The invariance of PSWFs with respect to the Fourier transform and an application of the Fourier convolution theorem yields the Hilbert transform of PSWFs in the form of a finite Fourier integral which may be evaluated easily by quadrature. The probability distribution of the envelope may again be evaluated explicitly using the theory of characteristic functions.

## **Joint Extreme Statistics of Wave and Wind Loads on Offshore Wind Turbines**

Offshore wind turbines based on fixed foundations or supported by floaters are exposed both to wind and wave loads. Their analysis and design therefore presents an increased level of complexity since models of the wind loads on the turbine must be coupled with models for the wave loads on the supporting structure. This task has been undertaken for floating wind turbines by Sclavounos et. al. (2010) and Tsouroukdissian et. al. (2011).

The design of offshore wind turbines also requires models for the joint extreme statistics of the wave and wind loads exerted on the structure in severe weather environments. The wind speed profile at hub height and the associated seastate elevation are correlated and this correlation must be modeled and taken into account in the design of the offshore wind turbine. The number of sources of uncertainty governing the wind and wave environments is greater than that governing each individually. Therefore the development of a joint-KL representation of the stochastic wind and wave loads that takes into account their correlation and leads to a minimum number of independent wind-wave sources of uncertainty would be very valuable.

Stochastic wind speeds are described by well understood spectra and experimental data exist that contain information about the covariance structure of wind speeds and seastate elevation. These attributes may be used to develop a joint wind-wave KL representation of a particular environment extending the methods developed in the present article. The auto-correlation function of wind speeds and their averages may be estimated from the Fourier transform of the Von Karman or Kaimal spectra that are routinely used by the wind energy industry. The rate of decay of the resulting auto-correlation function with increasing time lag is exponential-like and conforms to a multi-step auto-regressive process. The KL representation of wind speeds may be carried out by starting from the KL expansion of the autocorrelation of wind speeds averaged over selected intervals. Such KL expansions are available in closed form for autocorrelation functions with exponential like decay. Their explicit orthogonal eigenfunctions may be used as the basis function set for the derivation of the KL representation of wind speeds with more general but similar auto-correlation functions, in a manner analogous to the use of the *sinc* function for ocean waves described above. An analogous process may be followed for the

derivation of the KL representation of the loads on wind turbine rotors obtained using standard computer programs.

Following the derivation of the KL representations of the wave loads on the fixed or floating foundation and the wind loads on the rotor, their statistical correlation may be studied by using the canonical correlation analysis discussed in Anderson (2003). The canonical correlation analysis leads to a parsimonious statistical model of the joint wave and wind loads on offshore wind turbines and their joint extreme statistics for use in design.

## **Forecasting of Seastate Elevation Records and Vessel Responses**

The ability to forecast wave elevation records and the responses of ships, offshore structures, floating wind turbines and wave energy converters has a wide range of applications for the safe operation of marine structures and the enhancement of the energy yield of ocean energy systems. Wave elevation records can be forecasted reliably several periods into the future in seastates which are reasonably narrow banded using multi-step autoregressive methods [Fusco and Ringwood (2010)]. The parsimonious KLS representation of ocean wave elevation records developed in the present article allows the derivation of explicit expressions the minimum number of auto-regressive coefficients necessary to predict the wave elevation record into the future and over a time window of interest for each particular application. This is the result of the optimality of the Karhunen-Loeve expansion and the selection of the optimal Slepian frequency. The coefficients of the auto-regressive model follows from the explicit solution of the Yule-Walker equations discussed in Box, Jenkins and Reinsel (2008) using the representation of the KLS representation auto-correlation function in terms of PSWFs discussed above. In the present forecasting problem knowledge of the signal is assumed over a finite time interval  $T$ . When the time interval  $T$  is infinite the solution of the forecasting problem has been given by Wiener (1949). In the case of non-stationary seastates the forecasting method described above may be generalized to account for time-dependent and stochastic coefficients using a state space representation and Kalman filtering as described in Durbin and Koopman (2001).

Applications of auto-regressive forecasting models of seastate elevations and vessel responses include the prediction of ship responses in severe seastates in order to prevent excessive motions, ship-to-ship or ship-to-offshore-platform loading operation, the enhancement of the energy yield of compliant Tension-Leg-Platform floating wind turbines via the feed-forward control of the wind turbine blade pitch angle and the development of optimal algorithms for the maximization of the yield of wave energy converters.

## 7. Acknowledgements

I would like to thank Yeunwoo Cho and Thomas Luybaert for their programming assistance. This research has been supported by Enel, b\_Tec and Alstom. Enel and b\_Tec are members of the MIT Energy Initiative. This financial support is greatly appreciated.

## 8. References

Anderson, T. W. (2003). *An Introduction to Multivariate Statistical Analysis*. Third Edition. Wiley Series in Probability and Statistics.

Basilevsky, A. (1994). *Statistical Factor Analysis and Related Methods. Theory and Applications*. Wiley Series in Probability and Mathematical Statistics.

Box, G. E. P., Jenkins, G. M and Reinsel, G. C. (2008). *Time Series Analysis. Forecasting and Control*. Fourth Edition. Wiley.

Durbin, J. and Koopman, S. J. (2001). *Time Series Analysis by State Space Methods*. Oxford Statistical Science Series. Oxford University Press.

Fusco, F. and Ringwood, V. J. (2010). Short-Term Wave Forecasting for Real-Time Control of Wave Energy Converters. *IEEE Transactions on Sustainable Energy*, Vol. 1, No. 2.

Kac, M. and Siegert, A. J. F. (1947). On the Theory of Noise in Radio Receivers with Square Law Detectors. *Journal of Applied Physics*, 18, 383-397.

Kiureghian, A. D. (2000). The Geometry of Random Vibrations and Solutions by FORM and SORM. *Probabilistic Engineering Mechanics* 15, 81-90.

Moore, I. C. and Cada, M. (2004). Prolate Spheroidal Wave Functions, an Introduction to the Slepian Series and its Properties. *Applied Computational Harmonic Analysis*, 16, 208-230.

Ochi, M. K. (1998). *Ocean Waves*. The Stochastic Approach. Cambridge University Press.

Rice, S. O. (1944). Mathematical Analysis of Random Noise. *Bell System Technical Journal*, 23, 282-332.

Rice, S. O. (1945). Mathematical Analysis of Random Noise. *Bell System Technical Journal*, 24, 46-156.

Sclavounos, P. D. (2011). The Impulse of Ocean Waves on Floating Bodies. To appear.

Sclavounos, P. D., Lee, S., DiPietro, J. (MIT), Potenza, G., Caramuscio, P. and De Michele G. (ENEL) (2010). Floating Offshore Wind Turbines: Tension Leg Platform and Taught Leg Buoy Concepts Supporting 3-5 MW Wind Turbines. European Wind Energy Conference EWEC 2010, Warsaw, Poland, April 20-23.

Slepian, D. and Pollack, H. O. (1961). Prolate Spheroidal Wave Functions, Fourier Analysis and Uncertainty - I, *Bell System Technical Journal*, 40, 43-63.

Tsouroukdissian, A. R., Fisas, A., Pratts, P. (ALSTOM) and Slavounos, P. D. (MIT) (2011). Floating Offshore Wind Turbines: Concept Analysis. American Wind Energy Association WINDPOWER 2011 Conference and Exhibition, Anaheim CA, May 22-25.



Wiener, N. (1949). *Extrapolation, Interpolation and Smoothing of Stationary Time Series*. John Wiley and Sons, Inc., New York.

Wiener, N. (1958). *Nonlinear Problems in Random Theory*. MIT Press.

Winterstein, S. R. (1988). Nonlinear Vibration Models for Extremes and Fatigue. *Journal of Engineering Mechanics*, 114, 10, 1772-1790.

Xiao, H., Rokhlin, V. and Yarvin, N. (2001). Prolate Spheroidal Wave Functions, Quadrature and Interpolation. *Inverse problems*, 17, 805-838.